New type of ruthenium sensitizers with a triazole moiety as a bridging group

Sanghyun Paek [a], Chul Baik [a], Moon-sung Kang [b], Hongsuk Kang [c], Jaejung Ko [a,*]

[a] Department of New Material Chemistry, Korea University, Jochiwon, Chungnam 339-7000, Republic of Korea
[b] Energy and Environment Lab, Samsung Advanced Institute of Technology, Yongin 446-712, Republic of Korea
[c] Department of Nano and Advanced Materials, College of Engineering, Jeonju University, Jeonju, Republic of Korea

ABSTRACT

A new type of ruthenium sensitizers **JK-91** and **JK-92** with a triazole moiety as a bridging group were designed and synthesized in an attempt to increase the π-conjugated system. Two compounds work as highly efficient sensitizers for the dye-sensitized nanocrystalline TiO_2 solar cell. Under standard AM 1.5 sunlight, the sensitizer **JK-91** yielded a short-circuit photocurrent density of 12.55 mA/cm^2, an open-circuit voltage of 0.73 V, and a fill factor of 0.73, corresponding to an overall conversion efficiency of 6.75%.

© 2010 Elsevier B.V. All rights reserved.

1. Introduction

Dye-sensitized solar cells (DSSCs) are attracting widespread interest as low-cost alternatives to conventional solid-state photovoltaic device because of their low-cost and high performance [1–3]. In these cells, the sensitizer is one of the key elements for high-power conversion efficiencies. Current high efficiency of DSSCs achieves with the sensitizer **N719** (*cis*-bis(isothiocyanato)bis(2,2′-bipyridyl-4,4′-dicarboxylato)ruthenium-(II)bis(tetrabutyl-ammonium) [4,5]. However, the main drawback of the **N719** sensitizer is the lack of absorption in the red region of the visible spectrum. One of the approaches to address these issues would be to substitute one of the 2,2′-bipyridyl-4,4′-dicarboxylate groups in the sensitizer into the conjugated bipyridine of the ancillary ligand [6–10]. This not only exhibits an intense and red-shifted peak of the sensitizer but also increases its hydrophobicity, stabilizing device performance under long-term light soaking. Using this concept, several Ru polypyridyl complexes have achieved power conversion efficiencies of 10–11% [11–14]. Nevertheless, the quest for new sensitizers that efficiently harvest solar light still continues to be an important issue. As small structural variation of sensitizers results in significant changes in redox energies and photo-physical properties, affecting dramatically the performance of DSSCs [15–18], judicious tuning of the LUMO and HOMO energy levels of sensitizer [19], panchromatic sensitization on TiO_2, and increasing of the molar absorption coefficient of sensitizer [20–23] are the strategies to be pursued in the molecular engineering of sensitizer.

In line with the continuation of the efforts in this direction for improving the power conversion efficiency, we have synthesized a new type of the ruthenium sensitizer, consisting of triazole moiety as a bridging group synthesized using click chemistry. The general idea is to use the triazole group for extending the π-conjugated backbone. In this article, we report the synthesis, characterization, and photovoltaic properties of a new type of ruthenium(II) complexes **JK-91** and **JK-92**.
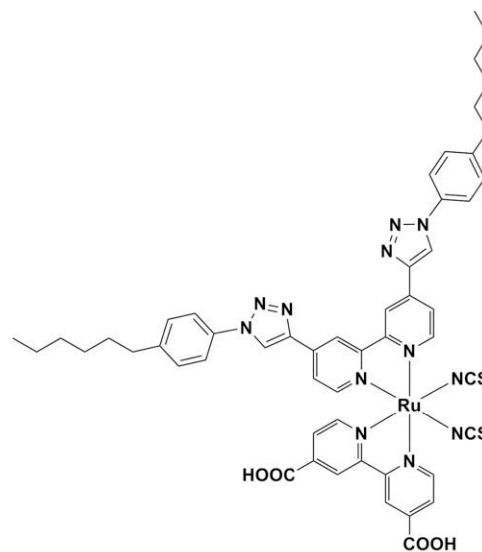
JK-91

* Corresponding author. Tel.: +82 41 860 1337; fax: +82 41 867 5396.
E-mail address: jko@korea.ac.kr (J. Ko).
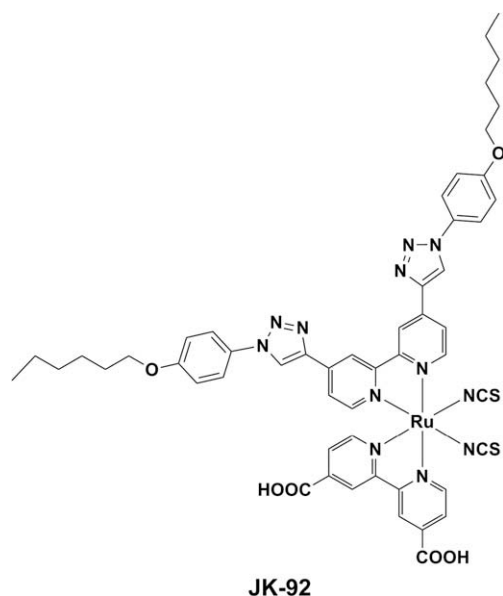
JK-92

2. Results and discussion

The synthetic procedures of ruthenium sensitizers **JK-91** and **JK-92** are outlined in Scheme 1. The ligands 3 and 4 were synthesized by the copper(I)-catalyzed click chemistry between a bis-alkyne and azides [24]. The reaction of [Ru(p-cymene)Cl₂]₂ complex with **3** or **4** in DMF under nitrogen resulted in the formation of a mononuclear complex. The hetero-leptic dichloro complexes were synthesized by reaction of the mononuclear intermediate with

4,4′-dicarboxyl-2,2′-bipyridine. The chloro intermediates reacted with a large excess of ammonium thiocyanate to afford the ruthenium sensitizers **JK-91** and **JK-92** (Scheme 1). The sensitizers **JK-91** and **JK-92** were spectroscopically characterized, and all data are consistent with the formulated structures.

The UV–Vis and emission spectra of **JK-91** and **JK-92** in DMF are shown in Fig. 1, together with the UV–Vis spectra of the corresponding dyes adsorbed on TiO₂ film. The absorption spectrum of **JK-91** exhibits two visible absorption bands at 388 and 529 nm, which are assigned as the metal-to-ligand charge transfer (MLCT) bands. Under the same conditions the sensitizer **JK-92** that contains the hexyloxy group instead of hexyl group causes a blue shift to 521 nm and a slightly narrow peak relative to the **JK-91**. The molar extinction coefficients of the low energy MLCT bands in **JK-91** (ε = 16,100 dm³ mol⁻¹ cm⁻¹) and **JK-92** (ε = 15,500 dm³ mol⁻¹ cm⁻¹) are higher than that of **N719** (ε = 14,700 dm³ mol⁻¹ cm⁻¹) [25].

The enhanced molar extinction coefficients of both sensitizers are attributable to the extension of the π-conjugation in the ancillary ligand. Anchoring of **JK-91** and **JK-92** on TiO₂ film was observed to broaden the absorption spectrum and to red shift the absorption threshold up to 730 nm. Similar broadening and red shift have been observed in other ruthenium sensitizers on TiO₂ films [26]. We observed that the sensitizers **JK-91** and **JK-92** exhibited strong luminescence maxima at 753 and 763 nm, respectively, when they are excited within their MLCT bands in an air-equilibrated solution at 298 K.

The cyclic voltammograms of **JK-91** and **JK-92** on TiO₂ films in CH₃CN with 0.1 M tetrabutylammonium hexafluorophosphate show quasi-reversible couples at 0.87 and 0.93 V vs. NHE, respectively (Fig. 2). The ground state redox potential of both sensitizers is higher than that of the iodide electron donor, providing a thermodynamic driving force for efficient dye regeneration. The reduction potential of two sensitizers calculated from the oxidation potential and the E_{0-0} determined from the intersection of normalized absorption and emission spectra is listed in Table 1. The excited-state redox
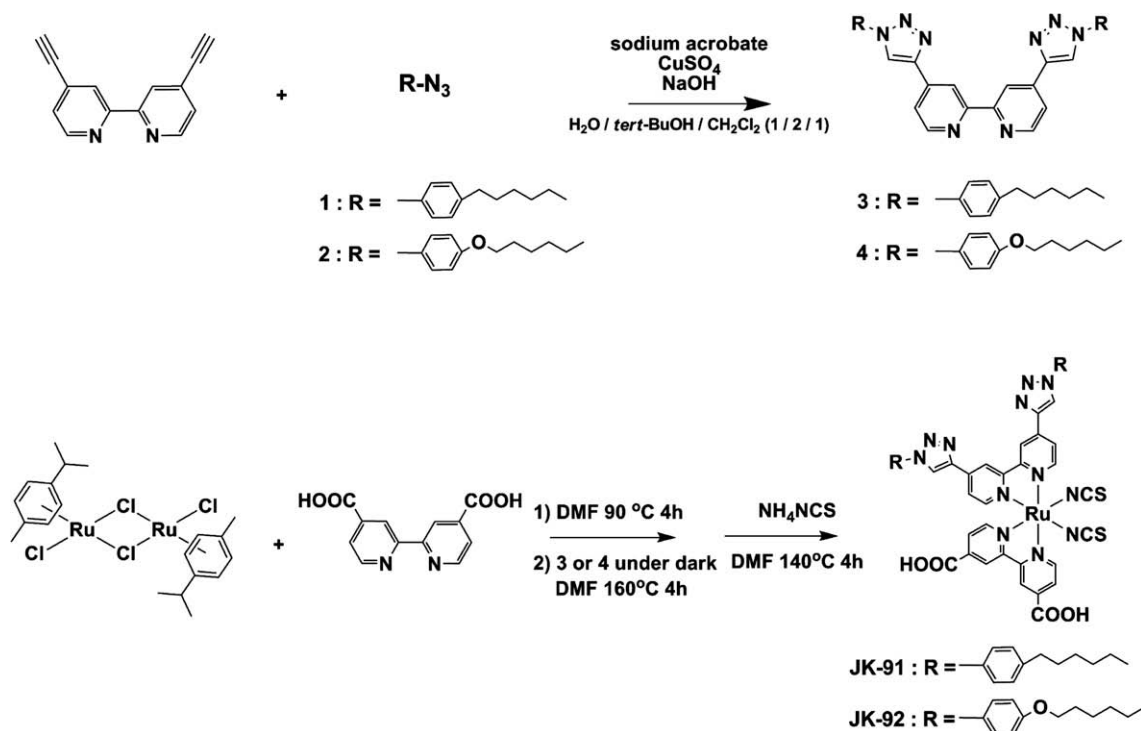
Scheme 1. Schematic diagram for the synthesis of ruthenium sensitizers **5** and **6**.
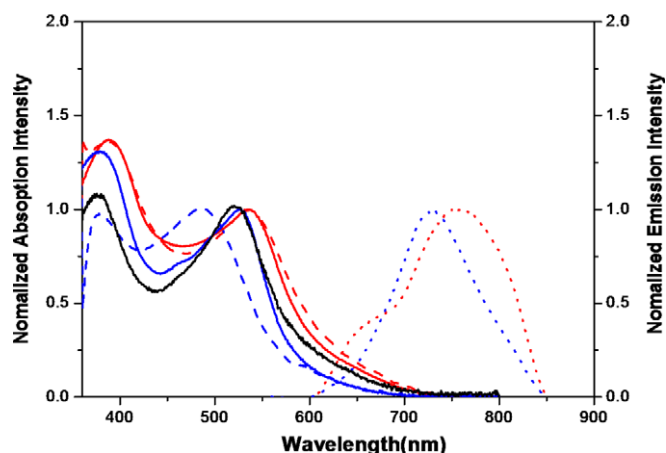
Fig. 1. Absorption spectra of **JK-91** (red solid line), **JK-92** (blue solid line) and **N719** (block solid line) in DMF, together with the absorption spectra of **JK-91** (red dash line) and **JK-92** (blue dash line) adsorbed on TiO₂ film and their emission spectra of **JK-91** (red dot line) and **JK-92** (blue dot line). (For interpretation of the references to colour in this figure legend, the reader is referred to the web version of this article.)
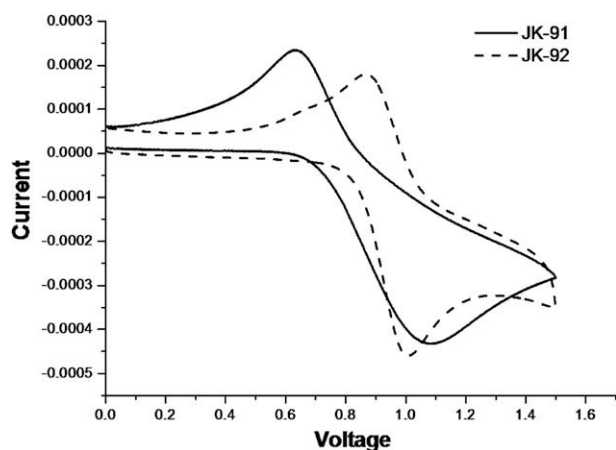

Fig. 2. CV of **JK-91** (solid line) and **JK-92** (dash line) on TiO₂ film with 0.1 M (*n*-C₄H₉)₄NPF₆ acetonitrile solution (scan rate of 50 mV s⁻¹).

potentials, $\Phi^0(S^+/S^*)$, of the dyes (**JK-91**: −0.92 V; **JK-92**: −0.90 V vs. NHE) are much negative than the conduction band of TiO₂ at approximately −0.5 V versus NHE, providing enough driving force for electron injection [27–29]. A slightly positive shift in the reduction potential in **JK-91** compared to **JK-92** is due to more delocalization of the π-conjugated system on the ancillary ligand.

We carried out the molecular orbital calculation of **JK-91** and **JK-92** to gain insight into the photo-physical properties using the B3LYP/6-31G* as exchange correlation function and 3-21G* as a basis set (Fig. 3). The calculation illustrates that the filled frontier orbital (HOMO) of both sensitizers is mainly composed of Ru 4d orbital with a sizable contribution from the NCS ligand orbital. The LUMO of both sensitizers is π* orbital delocalized on the dcbpy ligand. Examination of the HOMO and LUMO of both sensitizers indicates that photoexcitation was directly charged from the ruthenium–NCS unit to the carboxy pyridine ligand bound to the TiO₂ surface.

Fig. 4 shows action spectra of monochromatic incident photo-to-current conversion efficiencies (IPCEs) for DSSCs based on **JK-91** and **JK-92** using an acetonitrile-based electrolyte (electrolyte: 0.6 M 3-hexyl-1,2-dimethyl imidazolium iodide, 0.05 M I₂, 0.1 M LiI, and 0.5 M 4-tert-butylpyridine). The IPCE of **JK-91** shows a plateau of over 60% from 430 to 620 nm, reaching the maximum of 76% at 528 nm. The photo-response of the cell extends up to 780 nm. The decline of the IPCE above 630 nm toward the red is caused by the decrease in the extinction coefficient of **JK-91** in that region. The **JK-91** sensitizer shows a relatively large photocurrent and broad IPCE relative to those of **JK-92**, which is consistent with the absorption spectra of **JK-91** and **JK-92**. Under a standard global AM 1.5 solar condition, **JK-91** and **JK-92** sensitized cell gave a short circuit photocurrent density (J_{sc}) of 12.55 and 11.41 mA cm⁻², an open circuit voltage (V_{oc}) of 0.73 and 0.73 V and a fill factor of 0.73 and 0.74, corresponding to an overall conversion efficiencies η of 6.75 and 6.22%, respectively (Fig. 5). Under the same condition, the **N719** sensitized cell gave a J_{sc} of 14.68 mA cm⁻², a V_{oc} of 0.75 V and a fill factor of 0.73, corresponding to η of 8.06% (Table 1). Of particular importance is the 1.14 mA cm⁻² increase in **JK-91** relative to **JK-92**. To clarify the high photocurrent of **JK-91** sensitized cell compared to the **JK-92** sensitizer, we have measured the amount of dyes adsorbed on TiO₂ film. The adsorbed amounts of 2.6×10^{-7} mmol cm⁻² for **JK-91** and 2.7×10^{-7} mmol cm⁻² for **JK-92** are observed. Therefore, it is assumed that the enhanced photocurrent in **JK-91** is originated from a broad and intense absorption spectrum rather than their adsorbed amounts.

Fig. 5 shows the electron diffusion coefficients and lifetimes of the DSSCs employing different dyes (i.e. **JK-91**, **JK-92** and **N719** respectively.) displayed as a function of the J_{sc} and V_{oc}, respectively. No significant differences among the D_e values were seen at the identical short-circuit current conditions, meaning that the structural changes in the dye molecules are not the important factor dominating the electron diffusivity through nanocrystalline TiO₂ film [34]. In the case of the τ_e values, however, the significant difference was observed among the cells employing different dyes. The order of magnitude of the τ_e values was well consistent with that of the V_{oc} as shown in Table 1. The results demonstrate that

Table 1
Optical, redox and DSSC performance parameters of dyes.

Dye	λ_{abs}[a]/nm (ε/M⁻¹ cm⁻¹)	λ_{em}[b]/nm (ε/M⁻¹ cm⁻¹)	E_{ox}[c]/V	E_{0-0}[d]/V	E_{LU}[e]/V	J_{sc}[f] (mA/cm²)	V_{oc}[g] (V)	F.F[h]	η[i] (%)
JK-91	388(22,000) 529(16,100)	753	0.87	1.79	−0.92	12.55	0.73	0.73	6.75
JK-92	384(21,500) 521(15,500)	763	0.93	1.83	−0.90	11.41	0.73	0.74	6.22
N719						14.68	0.75	0.73	8.06

[a] Absorption spectra were measured in ethanol.
[b] Emission spectra were measured in ethanol.
[c] E_{ox} is oxidation potential. Red-ox potential of dyes on TiO₂ were measured in CH₃CN with 0.1 M (*n*-C₄H₉)₄NPF₆ with a scan rate of 50 mV s⁻¹ (vs. Fc/Fc⁺).
[d] E_{0-0} is voltage of intersection point between absorption and emission spectra. E_{0-0} was determined from intersection of absorption and emission spectra in ethanol.
[e] E_{LUMO} was calculated by $E_{ox} - E_{0-0}$.
[f] J_{sc}: short photocurrent density.
[g] V_{oc}: open-circuit photovoltage.
[h] FF: fill factor.
[i] η: total power conversion efficiency.

Fig. 3. Isodensity surface plots of the HOMO and LUMO of **JK**-**91** and **JK**-**92**.
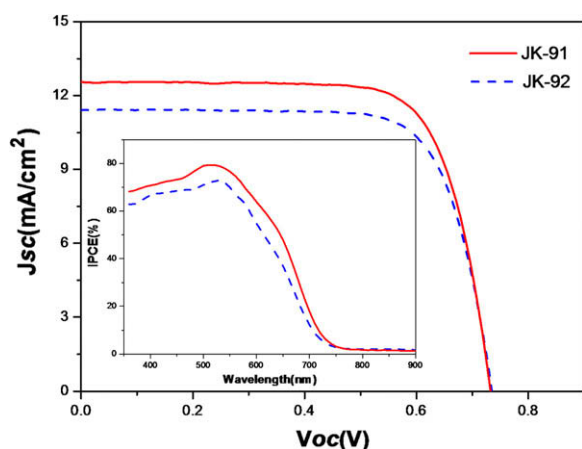

Fig. 4. I–V curves and IPCE spectra for **JK**-**91** (red solid line) and **JK**-**92** (blue dash line). (For interpretation of the references to colour in this figure legend, the reader is referred to the web version of this article.)

the introduction of hydrophobic alkyl chains could effectively retard the electron recombination originated from the direct contact between the electrons on TiO$_2$ surface and I$_3^-$ ions in electrolyte. However, the Ru-complex dyes showed the V_{oc} and τ_e values lower than those of **N719** owing to their bulky structures inducing the aggregation among the dye molecules during the adsorption onto TiO$_2$ surface.

3. Conclusion

In summary, we have synthesized new efficient ruthenium dyes **JK-91** and **JK-92** containing the triazol-4-yl unit by click chemistry that not only enhances the molar extinction coefficient but also shifts to the red region. The power conversion efficiency of the DSSCs based on the **JK-91** and **JK-92** reaches 6.22 and 6.75%. The power conversion efficiency was sensitive to the substituent unit. Alkyl introduction of dye in both sensitizers the V_{oc} due to the blocking effect of the charge recombination. The low photocurrent of **JK-91** and **JK-92** relative to that of **N719** is due to the low adsorbed quantity of two sensitizers. We believe that the development of efficient ruthenium sensitizers will be possible through the structural modifications of ancillary group.

4. Experimental section

4.1. General methods

All reactions were carried out under an argon atmosphere. Solvents were distilled from appropriate reagents. All reagents were purchased from Sigma–Aldrich, TCI and Acros Organics. ^{1}H NMR
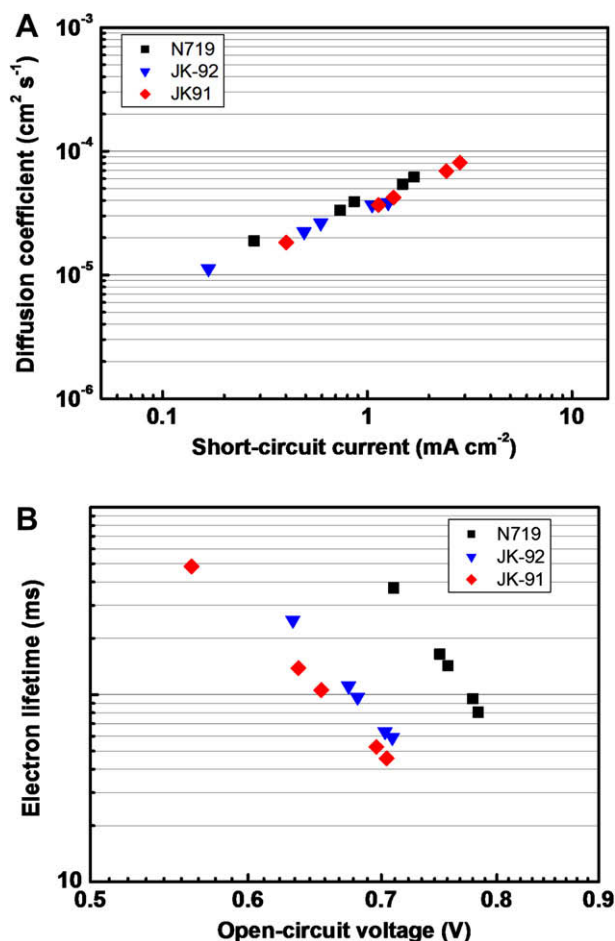

Fig. 5. Electron diffusion coefficients (A) and lifetimes (B) in the photoelectrodes adsorbing different dyes (i.e., **JK-91**, **JK-92** and **N719**).

and ^{13}C NMR spectra were recorded on a Varian Mercury 300 spectrometer. Elemental analyses were performed with a Carlo Erba Instruments CHNS-O EA 1108 analyzer. Mass spectra were recorded on a JEOL JMS-SX102A instrument. The absorption and photoluminescence spectra were recorded on a Perkin–Elmer Lambda 2S UV–vis spectrometer and a Perkin LS fluorescence spectrometer, respectively.

Cyclic voltammogram was carried out with a BAS 100B (Bioanalytical System, Inc.). A three electrode system was used and consisted of a gold disk, working electrode, and a platinum wire electrode. Redox potential of dyes on TiO$_2$ was measured in CH$_3$CN with a scan rate at 50 mV s^{-1} (vs. Fc/Fc$^+$).

4.2. Fabrication of DSSC

For the preparation of DSSC, a washed FTO (Pilkington, 8 Ωs q^{-1}) glass plate was immerged in 40 mM TiCl$_4$ aqueous solution as reported by the Grätzel group. The first TiO$_2$ layer of 7 μm thickness was prepared by screen printing with transparent mesoporous TiO$_2$ paste (13 nm anatase, solaronix), and the second opaque layer of 4 μm thickness (400 nm, CCIC) was coated for the purpose of light scattering. The TiO$_2$ electrodes were immersed into the dyes (**JK-91**, and **JK-92**) solutions (0.3 mM in DMF containing 10 mM 3a,7a-dihydroxy-5b-cholic acid) and kept at room temperature for 18 h. Counter electrodes were prepared by coating with a drop of H$_2$PtCl$_6$ solution (2 mg Pt in 1 mL ethanol) on a FTO plate. The electrolyte was then introduced into the cell, which was composed of 0.6 M 3-hexyl-1,2-dimethyl imidazolium iodide, 0.05 M iodine, 0.1 M LiI and 0.5 M 4-tert-butylpyridine in acetonitrile.

4.3. Characterization of DSSC

The cells were measured using 1000W xenon light source, whose power of an AM 1.5 Oriel solar simulator was calibrated by using KG5 filtered Si reference solar cell. The incident photon-to-current conversion efficiency (IPCE) spectra for the cells were measured on an IPCE measuring system (PV measurements).

4.4. Electron transport measurements

Electron diffusion coefficients and lifetimes were measured by the stepped light-induced transient measurements of photocurrent and voltages (SLIM-PCV). The transients were induced by a stepwise change in the laser intensity [30–33]. A diode laser (λ = 635 nm) as a light source was modulated using a function generator (UDP-303, PNCYS Co., Ltd., Korea). The initial laser intensity was 90 mW cm^{-2} constantly and less than 10% of the light intensity was turned down using a ND filter. The laser beam was positioned at the front side of the fabricated samples (0.04 cm^2). The laser was operated at the voltage of 3.0 V and stepped down to 2.9 V for 5 s. Then the single shot of the time-profiles of the photocurrent and photovoltage was obtained from an oscilloscope (TDS 3052B, Tektronix) through a current amplifier (SR570, Stanford Research Systems) and a voltage amplifier (5307, NF electronic Instruments), respectively. A total of 5 points were measured to determine the electron diffusion coefficients and lifetimes. For the measurement of SLIM-PCV, the TiO$_2$ thickness of the photoelectrode was controlled as approximately 10 μm.

4.5. Synthesis of sensitizers

4.5.1. Synthesis of 1-azido-4-hexylbenzene 1

To a three-necked flask tert-butyllithium (1.6 ml of 2.5 M solution in pentane, 4.1 mmol) and THF (30 ml) were charged under argon atmosphere at −78 °C. To this solution was dropwise added 1-

bromo-4-hexylbenzene (1 g, 4.1 mmol) dissolved in THF (10 ml) and stirred for 15 min at −78 °C. Then tosylazide (0.8 g, 4.1 mmol) dissolved in THF (10 ml) was added dropwise. During tosylazide addition the colour of the solution turned red. The reaction mixture was stirred for 14 h at −78 °C under argon atmosphere. A saturated solution of aqueous ammonium chloride (10 ml) was added dropwise at −78 °C and finally the reaction mixture was allowed to warm to room temperature. THF was removed by rotary evaporation and residue was extracted with Et$_2$O and washed with brine. The organic layer was dried over MgSO$_4$ and concentrated in vacuo. Column chromatography and recrystallisation (MeOH) afforded 4 as a light yellow solid. ^{1}H NMR (CDCl$_3$): δ 7.15 (d, 2H, ^3J = 8.1 Hz), 6.94 (d, 2H, ^3J = 8.1 Hz), 2.57 (t, 2H, ^3J = 6.6 Hz), 1.59 (m, 2H), 1.32 (m, 6H), 0.88 (t, 3H, ^3J = 6.6 Hz). ^{13}C NMR (CDCl$_3$): δ 158.3, 132.3, 116.4, 112.6, 35.5, 31.6, 29.2, 25.8, 22.7, 14.1. MS: m/z 202.27 [M+]. Anal. Calc. for C$_{12}$H$_{17}$N$_3$: C, 70.90; H, 8.43. Found: C, 70.68; H, 8.33.

4.5.2. Synthesis of 1-azido-4-(hexyloxy)benzene 2

The product was synthesized according to the procedure as described above for synthesis of 1. ^{1}H NMR(CDCl3): δ 6.94 (d, 2H, ^3J = 9 Hz), 6.87 (d, 2H, ^3J = 9 Hz), 3.92 (t, 2H, ^3J = 6.6 Hz), 1.76 (m, 2H), 1.34 (m, 6H), 0.91 (t, 3H, ^3J = 6.6 Hz). ^{13}C NMR (CDCl$_3$): δ 156.7, 132.2, 120.0, 115.8, 68.5, 31.7, 29.3, 25.8, 22.7, 14.1. MS: m/z 218.28 [M+]. Anal. Calc. for C$_{12}$H$_{17}$N$_3$O: C, 65.73; H, 7.81. Found: C, 65.93; H, 7.88.

4.5.3. Synthesis of 4,4′-bis(1-(4-hexylphenyl)-1H-1,2,3-triazol-4-yl)-2,2′-bipyridine 3

A three necked flask was charged with 4,4′-bis(ethynyl)-2,2′-bipyridyl (1 equiv.), the aryl azides 1 (2.2 equiv. per acetylene functionality), sodium ascorbate (0.1–0.2 equiv.), CuSO$_4$ (0.2 equiv.), NaOH (0.2 equiv.) and a solvent mixture of H$_2$O/tert-BuOH/CH$_2$Cl$_2$ (1/2/1). The flask was evacuated and flushed with argon twice. CuSO4 was added (stock solution, 10 mg CuSO$_4$ per 0.3 ml of water) and the mixture was stirred for 3 days at room temperature in the dark. After the acetylene starting material was consumed (TLC monitoring), the mixture was transferred into a separation funnel and CH$_2$Cl$_2$ was added. The aqueous phase was extracted with CH$_2$Cl$_2$. The organic phases were combined and washed with brine. After drying over MgSO$_4$, followed by filtration and removal of the solvent in vacuo, a colored solid was obtained that was purified by column chromatography to yield the respective products in high analytical purities. ^{1}H NMR(CDCl3): δ 8.81 (d, 2H, ^3J = 6 Hz), 8.80 (s, 2H), 8.51 (s, 2H), 8.09 (d, 2H, ^3J = 6 Hz), 7.72 (d, 4H, ^3J = 8.7 Hz), 7.37 (d, 4H, ^3J = 8.7 Hz), 2.70 (t, 4H, ^3J = 6.6 Hz), 1.66 (m, 4H), 1.33 (m, 12H), 0.90 (t, 6H, ^3J = 6.6 Hz). ^{13}C NMR (CDCl$_3$): δ 156.5, 150.1, 146.1, 144.5, 139.0, 134.7, 129.9, 120.6, 120.4, 119.7, 117.6, 35.5, 31.6, 29.2, 25.8, 22.7, 14.1. MS: m/z 609.78 [M+]. Anal. Calc. for C$_{38}$H$_{42}$N$_8$: C, 74.72; H, 6.93. Found: C, 74.52; H, 6.83.

4.5.4. Synthesis of 4,4′-bis(1-(4-(hexyloxy)phenyl)-1H-1,2,3-triazol-4-yl)-2,2′-bipyridine 4

The product was synthesized according to the procedure as described above for synthesis of 3. ^{1}H NMR(CDCl3): δ 8.81 (d, 2H, ^3J = 6 Hz), 8.80 (s, 2H), 8.45 (s, 2H), 8.09 (d, 2H, ^3J = 6 Hz), 7.68 (d, 4H, ^3J = 8.7 Hz), 7.06 (d, 4H, ^3J = 8.7 Hz), 3.92 (t, 4H, ^3J = 6.6 Hz), 1.76 (m, 4H), 1.34 (m, 12H), 0.90 (t, 6H, ^3J = 6.6 Hz). ^{13}C NMR (CDCl$_3$): δ 156.7, 150.1, 146.1, 144.5, 139.0, 132.2, 129.9, 120.6, 120.4, 119.7, 117.6, 68.3, 31.7, 29.3, 25.8, 22.7, 14.1, MS: m/z 641.79 [M+]. Anal. Calc. for C$_{38}$H$_{42}$N$_8$O$_2$: C, 71.00; H, 6.59. Found: C, 70.80; H, 6.49.

4.5.5. Synthesis of cis-[Ru(R₃)(H₂dcbpy)(NCS)₂] **JK-91**

[{RuCl(p-cymene)}₂] (0.188 mmol) was dissolved in DMF (30 mL) and **3** (2 equiv.) was added. The reaction mixture was heated at 80 °C under nitrogen for 4 h and then, 2,2′-bipyridine-4,4′-dicarboxylic acid (2 equiv.) was added. The reaction mixture was refluxed at 160 °C for another 4 h. Then an excess of NH₄NCS was added to the reaction mixture and heated at 130 °C for a further 5 h. The solvent was removed using a rotary-evaporator under vacuum. Water was added to the resulting semisolid to remove excess NH₄NCS. The water-insoluble product was collected on a sintered glass crucible by suction filtration and washed with distilled water, and diethylether. The crude complex was dissolved in a solution of tetra(n-butyl) ammonium hydroxide in methanol. The concentrated solution was charged onto a Sephadex LH-20 column and eluted with methanol. ^{1}H NMR(CDCl₃): δ 9.76 (s, 1H), 9.58 (s, 1H), 9.45 (d, 1H, ^3J = 5.8 Hz), 9.32 (d, 1H, ^3J = 6 Hz), 9.25 (s, 1H), 9.15 (s, 1H), 9.07 (s, 1H), 8.98 (s, 1H), 8.41 (d, 1H, ^3J = 5.8 Hz), 8.28 (d, 1H, ^3J = 6 Hz), 7.91–7.44 (br, 12H), 2.65 (t, 4H, ^3J = 6.6 Hz), 1.57 (m, 4H), 1.28 (m, 12H), 0.91 (t, 6H, ^3J = 6.6 Hz). MS: m/z 1072.26 [M+]. Anal. Calc. for $C_{52}H_{50}N_{12}O_4RuS_2$: C, 58.25; H, 4.70. Found: C, 58.50; H, 4.60.

4.5.6. Synthesis of cis-[Ru(R₄)(H₂dcbpy)(NCS)₂] **JK-92**

The product was synthesized according to the procedure as described above for synthesis of **5**. ^{1}H NMR(CDCl₃): δ 9.73 (s, 1H), 9.55 (s, 1H), 9.47 (d, 1H, ^3J = 5.8 Hz), 9.32 (d, 1H, ^3J = 6 Hz), 9.28 (s, 1H), 9.15 (s, 1H), 9.10 (s, 1H), 8.98 (s, 1H), 8.38 (d, 1H, ^3J = 5.8 Hz), 8.31 (d, 1H, ^3J = 6 Hz), 7.97 (d, 1H, ^3J = 6 Hz), 7.91 (d, 2H, ^3J = 9 Hz), 7.80 (d, 2H, ^3J = 9 Hz), 7.68–7.65 (br, 3H), 7.20 (d, 2H, ^3J = 8.1 Hz), 7.15 (d, 2H, ^3J = 8.1 Hz), 3.92 (t, 4H, ^3J = 6.6 Hz), 1.76 (m, 4H), 1.34 (m, 12H), 0.90 (t, 6H, ^3J = 6.6 Hz). MS: m/z 1104.25 [M+]. Anal. Calc. for $C_{52}H_{50}N_{12}O_6RuS_2$: C, 56.56; H, 4.56. Found: C, 56.50; H, 4.60.

Acknowledgments

References

[1] B. O'Regan, M. Grätzel, Nature 353 (1991) 737–740.
[2] M.K. Nazeeruddin, A. Kay, I. Rodicio, R. Humphry-Baker, E. Muller, P. Liska, N. Vlachopoulos, M. Grätzel, J. Am. Chem. Soc. 115 (1993) 6382–6390.
[3] A.J. Frank, N. Kopidakis, Coord. Chem. Rev. 248 (2004) 1165–1179.
[4] M.K. Nazeeruddin, P. Péchy, T. Renouard, S.M. Zakkeruddin, R. Humphry-Baker, P. Comte, P. Liska, L. Cevey, E. Costa, V. Shklover, L. Spiccia, G.B. Deacon, C.A. Bignozzi, M. Grätzel, J. Am. Chem. Soc. 123 (2001) 1613–1624.
[5] P. Wang, S.M. Zakeeruddin, J.E. Moser, R. Humphry-Baker, P. Comte, V. Aranyos, A. Hagfelt, M.K. Nazeeruddin, M. Grätzel, Adv. Mater. 16 (2004) 1806–1811.
[6] C.-Y. Chen, S.-J. Wu, C.-G. Wu, J.-G. Chen, K.-C. Ho, Angew. Chem., Int. Ed. 45 (2006) 5822–5825.
[7] C.-Y. Chen, S.-J. Wu, J.-Y. Li, C.-G. Wu, K.-C. Ho, Adv. Mater. 19 (2007) 3888–3891.
[8] K.-J. Jiang, N. Madaki, J.-B. Xia, S. Noda, S. Yanagida, Chem. Commun. (2006) 2460–2462.
[9] F. Matar, T.H. Ghaddar, K. Walley, T. DosSantos, J.R. Durrant, B. O'Regan, J. Mater. Chem. 18 (2008) 4246–4253.
[10] D. Kuang, C. Klein, S. Ito, J.-E. Moser, R. Humphry-Baker, N. Evans, F. Duriaux, C. Grätzel, M.K. Nazeeruddin, M. Grätzel, Adv. Mater. 19 (2007) 1133–1137.
[11] Y. Chiba, A. Islam, Y. Watanabe, R. Komiya, N. Koide, L.Y. Han, Jpn. J. Appl. Phys. Part 2 45 (2006) L638–L640.
[12] M.K. Nazeeruddin, F. De Angelis, S. Fantacci, A. Selloni, G. Viscardi, P. Liska, S. Ito, T. Bessho, M. Grätzel, J. Am. Chem. Soc. 127 (2005) 16835–16847.
[13] Y. Cao, Y. Bai, Q. Yu, Y. Cheng, S. Liu, D. Shi, F. Gao, P. Wang, J. Phys. Chem. C 113 (2009) 6290–6297.
[14] F. Gao, Y. Wang, D. Shi, J. Zhang, M. Wang, X. Jing, R. Humphry-Baker, P. Wang, S.M. Zakeeruddin, M. Grätzel, J. Am. Chem. Soc. 130 (2008) 10720–10728.
[15] C.-Y. Chen, H.-C. Lu, C.-G. Wu, J.-G. Chen, K.-C. Ho, Adv. Funct. Mater. 17 (2007) 29–36.
[16] P. Wang, C. Klein, R. Humphry-Baker, S.M. Zakeeruddin, M. Grätzel, J. Am. Chem. Soc. 127 (2005) 808–809.
[17] D. Kim, M.-S. Kang, K. Song, S.O. Kang, J. Ko, Tetrahedron 64 (2008) 10417–10424.
[18] E.A.M. Geary, L.J. Yellowlees, L.A. Jack, I.D.H. Oswald, S. Parsons, N. Hirata, J.R. Durrant, N. Robertson, Inorg. Chem. 44 (2005) 242–250.
[19] P.A. Anderson, G.F. Strouse, J.A. Treadway, F.R. Keene, T.J. Meyer, Inorg. Chem. 33 (1994) 3863–3864.
[20] C. Lee, J.-H. Yum, H. Choi, S.O. Kang, J. Ko, R. Humphry-Baker, M. Grätzel, M.K. Nazeeruddin, Inorg. Chem. 47 (2008) 2267–2273.
[21] A. Abbotto, C. Barolo, L. Bellotto, F. De Angelis, M. Grätzel, N. Manfredi, C. Marinzi, S. Fantacci, J.-H. Yum, M.K. Nazeeruddin, Chem. Commun. (2008) 5318–5320.
[22] T. Bessho, E. Yoneda, J.-H. Yum, M. Guglielmi, I. Tavernelli, H. Imai, U. Rothlisberger, M.K. Nazeeruddin, M. Grätzel, J. Am. Chem. Soc. 131 (2009) 5930–5934.
[23] M.K. Nazeeruddin, P. Péchy, T. Renouard, S.M. Zakkeruddin, R. Humphry-Baker, P. Comte, P. Liska, L. Cevey, E. Costa, V. Shklover, L. Spiccia, G.B. Deacon, C.A. Bignozzi, M. Grätzel, J. Am. Chem. Soc. 123 (2001) 1613–1624.
[24] H.C. Kolb, M.G. Finn, K.B. Sharpless, Angew. Chem., Int. Ed. 40 (2001) 2004–2021.
[25] S.M. Zakeeruddin, M.K. Nazeeruddin, R. Humphry-Baker, P. Péchy, P. Quagliotto, C. Barolo, G. Viscard, M. Grätzel, Langmuir 18 (2002) 952–954.
[26] S.-R. Jang, C. Lee, H. Choi, J. Ko, J. Lee, R. Vittal, K.-J. Kim, Chem. Mater. 18 (2006) 5604–5608.
[27] A.M. Bond, G.B. Deacon, J. Howitt, D.R. Macfarlane, L. Spiccia, G. Wolfbauer, J. Electrochem. Soc. 146 (1999) 648–650.
[28] P. Wang, S.M. Zakeeruddin, J.-E. Moser, M. Grätzel, J. Phys. Chem. B 107 (2003) 13280–13285.
[29] K.-S. Chen, W.-H. Liu, Y.-H. Wang, C.-H. Lai, P.-T. Chou, G.-H. Lee, K. Chen, H.-Y. Chen, Y. Chi, F.-C. Tung, Adv. Funct. Mater. 17 (2007) 2964–2974.
[30] S. Nakade, T. Kanzaki, Y. Wada, S. Yanagida, Langmuir 21 (2005) 10803–10807.
[31] M.-S. Kang, K.-S. Ahn, J.-W. Lee, Y.S. Kang, J. Photochem. Photobiol. A: Chem. 195 (2008) 198–204.
[32] K.-S. Ahn, M.-S. Kang, J.-K. Lee, B.-C. Shin, J.-W. Lee, Appl. Phys. Lett. 89 (2006) 013103.
[33] K.-S. Ahn, M.-S. Kang, J.-W. Lee, Y.S. Kang, J. Appl. Phys. 101 (2007) 084312.
[34] K. Hara, K. Miyamoto, Y. Abe, M. Yanagida, J. Phys. Chem. B 109 (2005) 23776–23778.